Tikrit Journal of Engineering Sciences (2025); 32(1): 1538
DOI: http://doi.org/10.25130/tjes.32.1.8

IRAQI Academic Scientific Journals

ISSN: 1813-162X (Print); 2312-7589 (Online)
Tikrit Journal of Engineering Sciences
available online at: http://www.tj-es.com

TJES Tikrit Journal of Engineering Sciences

Friction Stir Spot Welding between Copper and AA6061-T6 with the Aid of Interlayer: An Experimental Study

Kareem A. Falih *, Isam J. Ibrahim, Sabah K. Hussein
Applied Mechanics Department, Technical Engineering College-Baghdad, Middle Technical University, Baghdad, Iraq.

Keywords:
Pure Copper; Keyhole problem; Aluminum alloys; Friction stir spot welding; IL-FSSW; Lap shear tensile.

Highlights:

- *Dissimilar metals were joined using the novel Friction Stir Spot Welding technology with the help of an intermediate layer.*
- *Tensile strength was increased using IL-FSSW compared to other technologies.*
- *The change in grain size fluctuated the microhardness.*
- *The results of the microstructure examination using an electron scanning microscope showed that the sample had suffered a brittle fracture.*

ARTICLE INFO
Article history:

Received	13 Aug. 2023
Received in revised form	26 Nov. 2023
Accepted	07 Jan. 2024
Final Proofreading	02 Sep. 2024
Available online	08 Mar. 2025

Citation: Falih KA, Ibrahim IJ, Hussein SK. **Friction Stir Spot Welding between Copper and AA6061-T6 with the Aid of Interlayer: An Experimental Study**. *Tikrit Journal of Engineering Sciences* 2025; **32**(1): 1538.
http://doi.org/10.25130/tjes.32.1.8

*Corresponding author:

Kareem A. Falih
Applied Mechanics Department, Technical Engineering College-Baghdad, Middle Technical University, Baghdad, Iraq.

Abstract: A commercial sheet of pure Copper (Cu) and an Aluminum alloy sheet (AA 6061-T6) were joined at a thickness of 2 mm using Friction Stir Spot Welding with an intermediate layer (IL-FSSW) with a pinless tool. The present work was conducted according to various parameters in terms of rotation speed, feed rate, soaking time, the stability of the plunge depth (2 mm), and the diameter of the welding tool (12 mm). The welding process parameters were optimized based on the Taguchi method, using the design of experiments (DOE). The results proved that the utmost shear force was fulfilled at a rotating speed of 1800 RPM, feed rate of 15 mm/min, soaking time of 20 sec, and shear force of 3908 N (Cu above Al sheet). Under the same arrangement of sheets, the maximum microhardness was 157Hv at 1120 rpm, 15 mm/min feed, 10 s soaking time, and 10 sec preheating in the stir zone (SZ). There was a change in the microstructure of the Weld spot and the base metal. The pictures showed the difference in the size of the crystalline grains of the cross-section of the weld joint and different zones. The microstructure was analyzed using light microscopy, scanning electron microscopy SEM, EDS, and XRD examination to determine the phases. The results showed a change in the grain size according to regions and that intermetallic compounds (IMCs) led to a brittle fracture in the welded samples.

لحام بقعة الاحتكاك بين صفيحة من النحاس النقي وصفيحة سبائك الالمنيوم (AA6061-T6) بمساعدة طبقة وسطية: دراسة تجريبية

كريم عباس فالح، عصام جبار إبراهيم، صباح خماس حسين
قسم الميكانيكا التطبيقية/ الكلية التقنية الهندسية-بغداد/ الجامعة التقنية الوسطى/ بغداد، العراق.

الخلاصة

في هذه الدراسة تم ربط صفيحة من معدن النحاس النقي وصفيحة من سبائك الالمنيوم AA6061-T6 بسمك ٢ ملم باستخدام لحام بقعة الاحتكاك بمساعدة الطبقة الوسطية مع اداة بدون دبابيس. تم اجراء هذا العمل وفقًا لمتغيرات مختلفة من حيث سرعة الدوران والتغذية ووقت السكون وثبات عمق الغطس (٢ ملم) وايضا قطر الأداة (١٢) ملم. تم تحسين معاملات عملية الاحتكاك بناء على طريقة تاغوتشي والاعتماد على تصميم التجارب. اظهرت النتائج المتحصلة إنه تم تحقيق أعلى قوة قص عند سرعة دوران ١٨٠٠ دوره في الدقيقة وعند معدل تغذية ١٥ ملم/دقيقة ووقت سكون ٢٠ ثانية حيث كانت قوة القص ٣٩٠٨ نيوتن (عند ترتيب صفيحة النحاس أعلى صفيحة الالمنيوم) وكانت عند نفس ترتيب الصفائح قيمة الصلادة الدقيقة (157Hv)عند سرعة دوران ١١٢٠ دورة في الدقيقة ومعدل تغذية ١٥ ملم/دقيقة ووقت سكون ١٠ ثانية ووقت تسخين مسبق ١٠ ثانيه ايضًا في منطقة التقليب. كذلك اظهرت صور البنية المجهرية للمقطع العرضي تغيرًا في حجم الحبيبات البلورية بين بقة اللحام والمعدن الرئيسي. تم تحليل البنية المجهرية باستخدام المجهر الضوئي ومجهر المسح الالكتروني SEM و EDS وفحص الأشعة السينية XRD لتحديد الاطوار. أظهرت النتائج تغيرًا في حجم الحبيبات وفقًا للمناطق، وكذلك اظهرت النتائج أن وجود المركبات المعدنية يؤدي الى الكسر الهش في العينات الملحومة.

الكلمات الدالة: سبائك الالمنيوم، النحاس النقي، لحام بقعة التقليب الاحتكاكي، مشكلة ثقب المفتاح، قص الشد التراكبي، لحام بقعة الخلط الاحتكاكي مع الطبقة الوسيطة.

1.INTRODUCTION

The scope of using Aluminum in manufacturing Automotive Structures has grown significantly due to its exceptional properties, such as low weight, high ductility, and high thermal and electrical conductivities. The challenge for researchers is connecting Aluminum to other metals. Therefore, they concentrated on solid-state welding as an alternative and optimal solution for joining dissimilar metals [1]. Aluminum and Copper are a significant combination that has prospective applications in various industrial domains due to the good properties of these two metals, high-quality bonding must be constructed between them [2]. Galvao et al. proved that solid-state welding is the most convenient method for joining Aluminum and Copper due to the significant difference in their coefficients of thermal expansion [3]. FSSW is the latest technology within solid-state welding processes, and it has been more efficient than conventional methods of joining dissimilar metals. Numerous studies have been conducted on this method by manufacturers of airplanes, trucks, trains, cars, and household appliances. This bonding method addresses most of the problems associated with Fusion welding when welding Al and Cu [1]. FSSW works using a non-consumable rotating tool, which descends on the workpiece vertically until contact, after which an axial force is applied for a specific period called dwell time. Through the rotational movement of the tool and friction with the workpiece, heat is generated, hardening the metal and forming the bonding joint. The mechanical properties and microstructure are controlled by multiple parameters, such as rotation speed, dwell time, and plunge depth [4, 5]. FSSW is used to bond wires, sheets, and terminals made of similar or dissimilar materials. Its purpose is to help the material retain its intrinsic metallic properties as much as possible, which are difficult to maintain when using welding, fusion, brazing, and soldering techniques. The processes mentioned above form intermetallic compounds between metals, which should be avoided using solid-state welding technology [6]. Akinlabi et al. investigated the relationship between electrical resistance and the generated heat when welding Al-Cu. They found that the high input heat increased the electrical resistance of the joints by 9.8% more than the base metal [7]. Savolainen found that the joint's resistance was higher than the average value of the two parent metals, with a percentage of 2.5% [8]. Akbari et al. studied the temperature difference between Aluminum and Copper for welding joints in two cases from sheet arrangement, Al/Cu or Cu/Al. They found that the temperature at the center of the welding surface for Cu/Al was lower when than Al/Cu due to the Copper thermal conductivity. The Cu/Al joint also showed the lowest shear tensile load at the same process parameters [9]. Wei et al. reported similar results. They noted that part of the Al alloy melted into Copper during welding. Defect-free joints can be obtained using FSSW conventional welding Al and Cu [10, 11]. Regensburg et al. used a fixed shoulder to reduce mixing at the interface, avoiding the defect of forming the hook and brittle metal compounds (IMCs) [12]. The presence of IMCs harms the tensile properties [13]. Chen et al. introduced ultrasound and zinc intermediate layer as bonding aids. They found that the FSSW strength has improved greatly; however, it was insufficient for engineering applications [14]. Zhou et al. measured the interface temperature of Al/Cu during FSSW. The peak temperature was 396 ^{O}C, 8 mm from the center of the welding spot, and a rotation speed of 2250 rpm [15]. Zhou et al. conducted further studies on FSSW. A high shear, tensile load

exceeding 4 kN was obtained for the Al/Cu at a rotational speed of 2000 rpm; however, the welding tool penetrated the lower sheet. However, the highest temperature at the joint Cu/Al interface, 8mm from the center of the welding spot, was 480^{0}C when the rotation speed was 1400 rpm. In addition, it increased the Cu/Al joint temperature because of the high melting point of copper. Cu/Al joint has enough strength bonding [16]. Gao et al. noted that obtaining a larger bonding area was easily done when forming a joint Cu/Al, which led to a high-quality joint [17]. Some disadvantages accompany the FSSW process when used in welding Aluminum and Copper, as follows:

1- Concavity in lower Al sheet: When the sheets are arranged by placing Copper on top of Aluminum, the upper hard Copper sheet presses on the lower soft Aluminum sheet, causing it to concave, leading to non-penetration of the interface of the joint Cu/Al [18].
2- Metallurgical reaction: The metal interactions at the interface between Aluminum and Copper affect the mechanical properties of the joint [19].
3- Insufficient mixing: An Aluminum Copper joint welded by FSSW, without an interlayer, may have insufficient mixing between the two metals, resulting in the formation of a partial joint at the interface [19].
4- Tooltip wearing: There are two challenges in friction welding of Aluminum and Copper: The tooltip wear and the hole the tool leaves on the workpiece reduce the welding quality [20].

By reviewing previous studies, it was found that the most significant defects affecting the weld joint performed by FSSW are the formation of fragile intermetallic compounds (IMCs) and a keyhole, leading to the concentration of stresses in the joint, which negatively affects the joint tensile strength and causes wear, so the researchers have been developing FSSW a technique to eliminate or reduce the defect of the keyhole. The intermediate layer friction stirs spot welding (IL-FSSW) technique by Bajilane [21]. This technique manufactures joints between similar and dissimilar sheets free from keyhole defects [21]. The present study used IL-FSSW technology to bond Aluminum alloys with pure Copper to produce a high-quality joint free from the keyhole defect associated with conventional FSSW technology. The mechanical properties were evaluated by testing the joint's shear, tensile strength, and hardness, while the microstructure was evaluated using the SEM, EDS, and XRD tests for the joint's cross-section. Up to date and according to the reported studies, no works still have used an intermediate layer of the same alloys to be joined with a new shape obtained via a traditional cutting process. However, previous research that used IL-FSSW technology in bonding similar and dissimilar metals used an intermediate layer that differs from the alloys to be bonded and had a disk shape with a certain diameter, meaning manufacturing special cutting dies to obtain the desired shape or using foil metals with a thickness of 0.05 microns obtained by the micro rolling process, or using nanomaterials, increasing in the cost and time required to complete the work. In the present work, the previously mentioned challenges were overcome using an intermediate layer of the same alloys to be bonded, and the polygonal shape obtained through the traditional cutting process was used without the need to manufacture special cutting molds or perform any additional operations. Also, the intermediate layer thickness was identical to the thickness of the alloys welded in this study, contrary to previous studies.

2.WELDING PROCEDURE

The technology of IL-FSSW mainly depends on adding an intermediate layer between the sheets to be welded. The main function of the intermediate interlayer is to prevent the occurrence of keyhole defects in the welding spot or its occurrence but shallowly. Figure 1 shows the main steps of the IL-FSSW technique. A milling machine with different rotation speeds was used to complete the work. The mold was made of stainless steel and consisted of two parts: the lower part, attached and fixed to the machine base, and the upper part, i.e., movable. The samples to be welded were fixed inside the mold after being cut according to the required standard dimensions. Figure 1 (a) shows the fixing workpieces cross-section and the intermediate interlayer inside the mold. An initial pressure force was exerted on the two sheets and the interlayer. This force formed a concave protrusion due to the penetration of the middle interlayer into the upper sheet, Fig. 1 (b). The welding tool was lowered to contact the surface of the upper sheet, and it rotated to produce a friction force between it and the workpiece. This friction produced heat that annealed metals and bound them together. During the tool rotation, additional compressive force was applied by feeding from the machine to obtain the plunge depth, Fig.1 (c- d). After the set dwell time, the tool was pulled up, leaving behind a welding spot with a shallow keyhole, Fig. 1 (e).

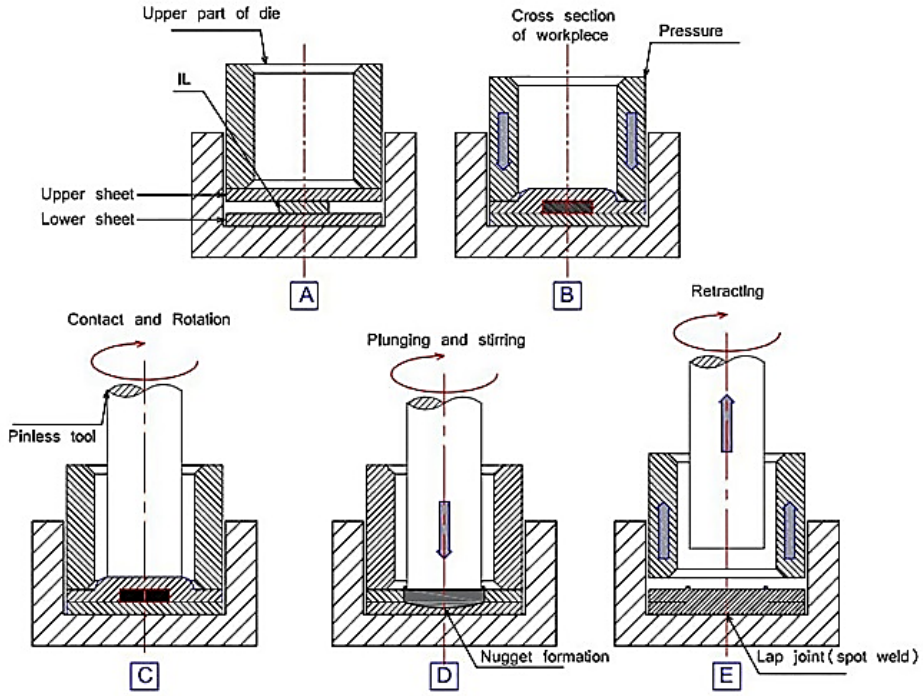

Fig. 1 The Main Steps of IL-FSSW.

3.EXPERIMENTAL SETUP

The materials used in this research were pure Cu and Aluminum alloy AA6061-T6, with a thickness of 2 mm. Tables 1-4 show the alloys' chemical composition and mechanical properties. Table 5 shows the chemical composition of a cylinder-shaped welding tool with a diameter of 12 mm. The variable parameters used in this experiment were rotation speed, feeding, dwell time, and preheating, see Table 6, as the plunge depth was fixed at 2 mm. The interlayer was taken from the same alloy to be bonded and ribbed with a dimension of 8×8×2 mm. The work plan was divided into four groups, as follows:

- Group B-1 (AA6061-T6/ pure Cu), IL of AA6061-T6 (8x8x2 mm).
- Group B-2 (AA6061-T6/ pure Cu), IL of Cu (8x8x2mm).
- Group B-3 (pure Cu / AA6061-T6), IL of AA6061-T6 (8x8x2 mm).
- Group B-4 (pure Cu / AA6061-T6), IL of Pure Cu (8x8x2 mm).

The levels and parameters used in this experiment are presented in Table 6.

4.DESIGN OF EXPERIMENT

The Taguchi method was used to design experiments (DOE). Where the variable parameters were placed in an orthogonal matrix (L9), as shown in Table 7. The Matrix was applied to the four previously mentioned work aggregates. The method of installing samples on the machine for work is shown in Fig. 2. Tensile test samples were prepared according to AWS Standard [25]. Figures 3-5 show the method of arranging the samples and the overlap distance between the samples in which the welding spot is visible.

Table 1 Chemical Composition of Aluminum AA6061-T6 (ASTM B209) [22].

Elements wt. Material	Si %	Fe %	Cu %	Mn %	Mg %	Cr %	Zn %	Ti %	Other	Al %
Standard	0.40-0.8	0.7	0.15-0.40	0.15	0.8-1.2	0.04-0.35	0.25	0.15	0.05-0.15	remainder
Actual	0.626	0.481	0.199	0.0554	0.936	0.138	0.0584	0.0276	0.058	97.2

Table 2 Chemical Composition of Pure Copper, S-Cu-5 DIN EN 1286 [23].

Elements wt. Material	Zn %	Pb %	Sn %	P %	Mn %	Fe %	Ni %	Sb %	S %	Al %	Bi %	Ti %	Cu%
Actual	----	----	0.0386	0.0449	----	0.0158	----	----	----	----	----	----	99.9

Table 3 Mechanical Properties of Aluminum Alloy AA6061-T6 (ASTM B209) [22].

Property Material		Ultimate stress σu (MPa)	Yield strength σY (MPa)	Elongation %
AA6061-T6	Normal	290	241	10
	Actual	326.18	293.36	16.25

Table 4 Mechanical Properties of Pure Copper (S-Cu-5 DIN EN 12861) [23].

Property Material		Ultimate stress σu (MPa)	Yield strength σY (MPa)	Elongation %
Cu-pure	Normal	220	69	45

Table 5 Chemical Composition of HSS Tool ASTM A 600-92a [24].

Elements wt. Material	Si	C	Cr	Mn	W	V	MO	P/S
Standard	0.20 - 0.45	0.88 – 0.85	3.75 – 4.50	0.15 – 0.40	5.50 – 6.75	1.75 – 2.20	4.50 – 5.50	0.03
Actual	0.464	0.908	5.14	0.203	0.833	0.667	1.06	0.5

Table 6 The Levels and the Parameters Used.

Parameter	Level 1	Level 2	Level 3
Rotation speed, N (RPM)	1120	1400	1800
Feed rate (mm/min)	15	20	25
Soaking time (sec)	10	15	20

Table 7 Shows the Experimental Design of the L9 Orthogonal Array.

Experimental NO.	Rotational Speed, RPM	Feed rate (mm/min)	Soaking time (sec)	Preheat Time (sec)
1	1120	15	10	10
2	1120	20	15	15
3	1120	25	20	20
4	1400	15	15	15
5	1400	20	20	20
6	1400	25	10	10
7	1800	15	20	20
8	1800	20	10	10
9	1800	25	15	15

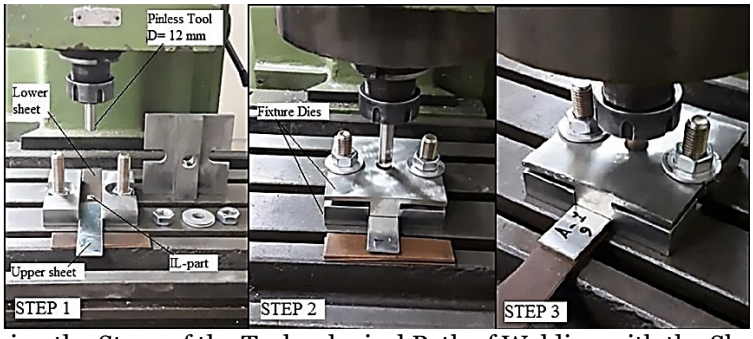

Fig. 2 Photos Showing the Steps of the Technological Path of Welding with the Shape of the Die Used.

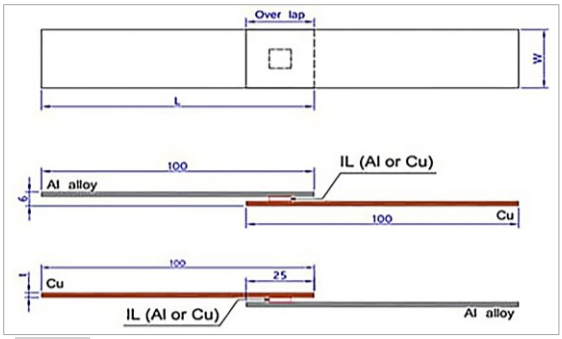

Fig. 3 The Arrangement of the Intermediate Layer and the Sheets to be Welded.

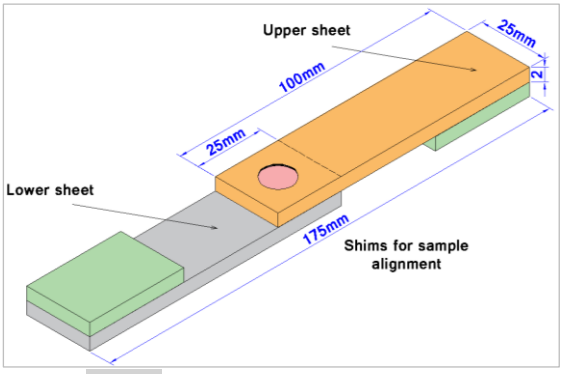

Fig. 4 Standard Tensile Sample.

Fig. 5 The External Appearance of the Welding Spot Surface.

5.TENSILE SHEAR TEST

All samples achieved bonding except the first group (B-1) samples, which did not achieve definitively. A tensile test was performed to determine the shear force that the joint endures, and the head speed of the tensile tester was 1 mm/min. The external appearance of the weld joint spot is shown in Fig. 5. The examination was conducted in the laboratory of the Materials Department, Engineering Technical College, Baghdad. The welded overlap sample dimensions were (25 mm wide and 175 mm long). To prevent the sample from slipping during testing, additional pieces were

installed on the edges of the sample having the same thickness as the base metal. Tables 8-10 show the tested samples' shear and tensile strength results. The results were evaluated to extract the ideal samples in each working group by Taguchi analysis.

Table 8 Group Tensile Test Results B-2.

Sample No.	Rotating Speed RPM	Feed Rate (mm/min)	Soaking Time (sec)	Preheat Time (sec)	Shear Failure Force (N) with IL
1	1120	15	10	10	0
2	1120	20	15	15	0
3	1120	25	20	20	1390
4	1400	15	15	15	774
5	1400	20	20	20	1409
6	1400	25	10	10	**2346**
7	1800	15	20	20	1521
8	1800	20	10	10	1829
9	1800	25	15	15	2338

Table 9 Group Tensile Test Results B-3.

Sample NO.	Rotating speed RPM	Feed rate (mm/min)	Soaking time (sec)	Preheat time (sec)	Shear failure force (N) with IL
1	1120	15	10	10	3652
2	1120	20	15	15	2972
3	1120	25	20	20	3292
4	1400	15	15	15	2614
5	1400	20	20	20	2451
6	1400	25	10	10	2888
7	1800	15	20	20	**3908**
8	1800	20	10	10	3137
9	1800	25	15	15	3372

Table 10 Group Tensile Test Results B-4.

Sample NO.	Rotating speed RPM	Feed rate (mm/min)	Soaking time (sec)	Preheat time (sec)	Shear failure force (N) with IL
1	1120	15	10	10	**3727**
2	1120	20	15	15	2718
3	1120	25	20	20	2330
4	1400	15	15	15	2625
5	1400	20	20	20	2313
6	1400	25	10	10	2839
7	1800	15	20	20	3332
8	1800	20	10	10	2710
9	1800	25	15	15	2322

After the evaluation, Taguchi analysis gave a new optimum sample in group B-2 with new parameters, i.e., 1800 rpm, 25 mm/sec Feed, 20 sec s.time, and without preheating. After the sample was welded and tested, it was exposed to a shear strength of 3132N with an increase of 25% over the highest sample in the group. In group B-3, sample 7 was the ideal sample chosen by the Taguchi analysis, and in group B-4, sample 1 was the optimum sample. The highest reading in the tensile test was achieved in sample 7 of group B-3 and was 3908 N. The resulting joint was assessed with the formula for finding the minimum failure stress of the Weld spot listed below, developed by the American Welding Society (AWS). It was then compared with the shear strength results from the tensile test. The equation was applied to the main minerals, and the maximum tensile strength was extracted, as shown in Table 11. By comparing the results, it was found that the maximum shear force resulting from the tensile test was lower than the maximum tensile stress for either Aluminum or Copper, which was calculated using the equation below to calculate the minimum lap shear failure force (*mLSFF*) [26-28]

$$mLSFF = \frac{(-6.36\times10^{-7}\times S^2+6.58\times10^{-4}\times S+1.674)\times S\times4\times t^{1.5}}{1000} \quad (1)$$

where S is the tensile stress of the base metal (the softer sheet), and t is sheet thickness. Table 11 shows the lowest shear force at which base metals fail, obtained by applying Eq. (1) [29].

Table 11 mLSFF of base metals used.

Base Metals Used	UTS (MPa)
AA6061-T6	6.719
Cu pure	4.886

Table 12 shows some of the researcher's findings and compares them with the results of the present study. The results indicated that the achieved tensile shear strength was higher than conventional FSSW.

Table 12 The Results of the Tensile Shear Force Resulting from the Bonding of Aluminum and Copper and Compared to the Present Study.

	Reference	Lap Configuration	Auxiliary Process	Tensile Shear Load (KN)	Year
1	Zuo et al. [30]	Cu / Al	Ultrasound	2.58	2021
2	Muna Khethier.[31]	Al/Cu	FSSW	2.29	2021
3	Hua et al. [2]	Cu / Al	Zn interlayer	3.32	2022
4	Current study	Cu /Al	IL- FSSW	3.9	------

Figure 6 shows the great bearing capacity of welds made using IL-FSSW technology compared to other studies using FSSW technologies.

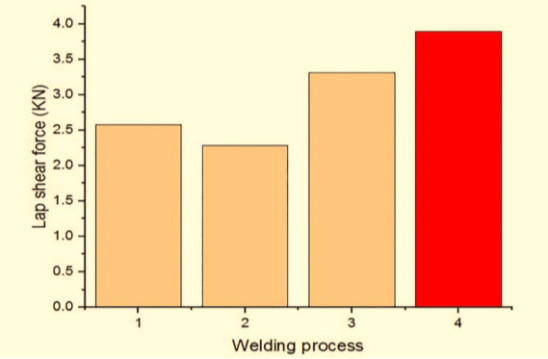

Fig. 6 A Comparison of the Tensile Results in the Present and Previous Studies.

6.MICROHARDNESS

The microhardness test was conducted at the Central Agency for Standardization and Quality Control-Baghdad, using a Vickers microhardness tester under a load of 50 g and a time of 15 sec. The distance between one indentation point and another was 1 mm along each line, according to the ISO 6507-1 specification. Forty-five test points were considered for one sample, distributed over three parallel lines on the sample cross-section. Figure 7 shows the technological path for conducting a microhardness examination. The examination was conducted on three samples representing the ideal samples in the work Groups B-2, B-3, and B-4. Figures 8-10 show the distribution of hardness values on the cross-section of the sample and in different areas, such as SZ, TMAZ, HAZ, and BM. Three lines were taken on the sample to measure the hardness and move away from the center of the welding spot at different distances. The first line moves away by a distance of 0,25 mm, the second of 0,75 mm, and the third of 1,25 mm, as is evident in Fig. 10. The results indicated that the highest value of microhardness was obtained in the optimum sample of group B-4 and estimated at 157 Hv at Rotating speed 1120 rpm, Feed rate 15 mm/min, s.time 10 sec, and preheat 10 sec. In addition, the achieved hardness value exceeded the hardness of the two base metals, measured by the Vickers micro-hardness device. The hardness for Aluminum AA6061-T6 was 107 Hv, and Copper's was 86.333 Hv.

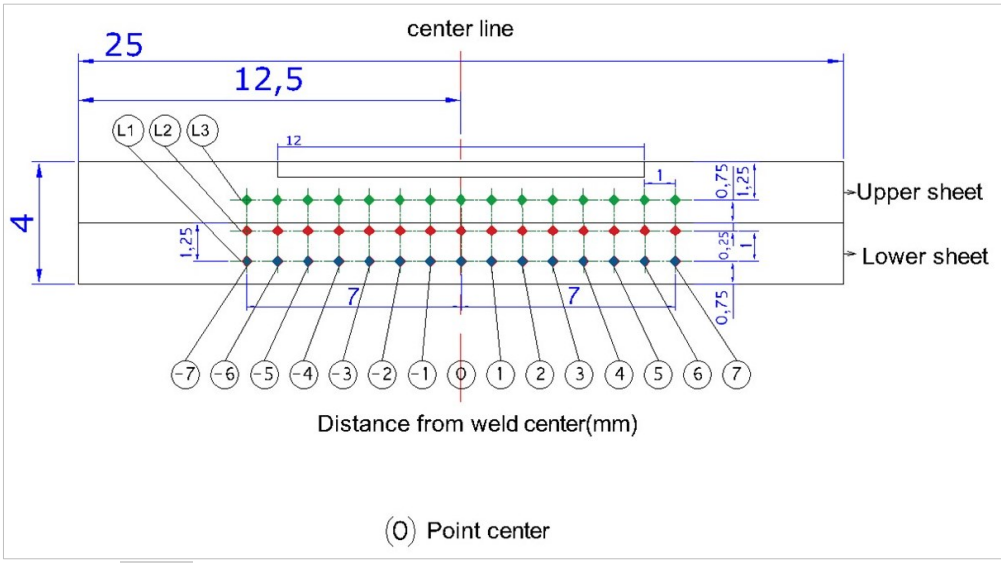

Fig. 7 The Technological Path of Examination of Microhardness.

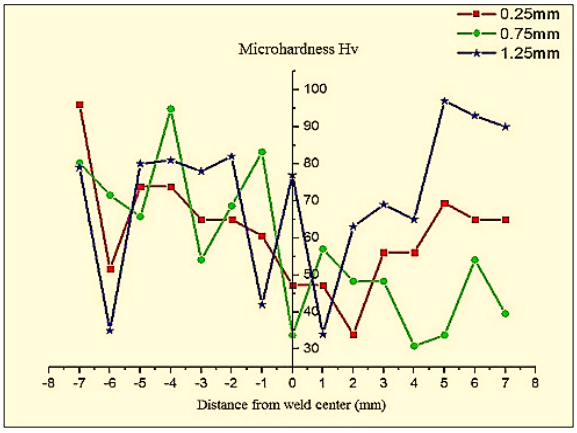

Fig. 8 Group B-2.

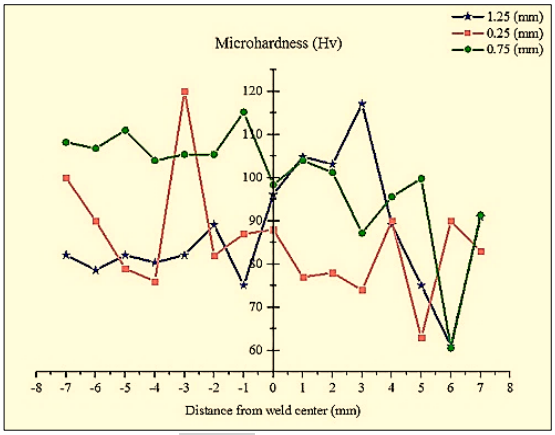

Fig. 9 Group B-3.

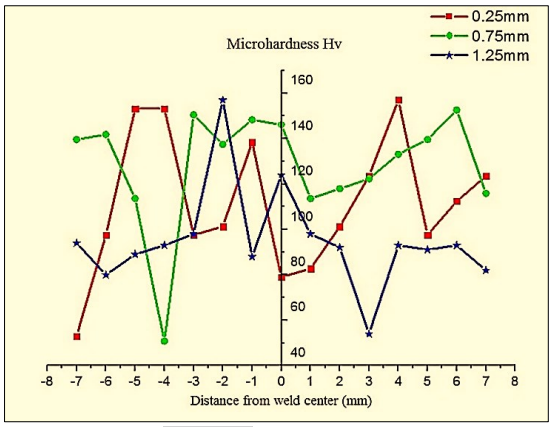

Fig. 10 Group B-4.

Figures 8-10 indicate a significant fluctuation in the hardness numbers. This difference in hardness results from the diversity in the microscopic structure of the weld nugget and the base metal, such as grain size, sediment, density, and intermetallic compounds. All this happened under pressure and temperature, both due to the welding tool, sometimes by pressure and another by friction [21].

7.MICROSTRUCTURAL ANALYSIS AND WELD GEOMETRY

The first welding steps began with the contact of the upper sheet using a rotary welding tool, which performed the preheating process; after the specified time had elapsed, the feeding process began to obtain the required plunged depth of 2 mm. To achieve the bonding between Aluminum and Copper, preheating was necessary due to the difference in thermal conductivity between the two metals, i.e., Al 237 w/mk and Cu 401 w/mk [32], and Copper's high ability to dissipate heat. From the tensile test results of all welding experiments, the bonding between the sheets was well achieved when the Copper sheet was placed on top of the Aluminum sheet. As the tool sinks along the center of the spot, pressure and friction alter the heating of the interlayer. It is responsible for forming the solid Nugget zone (NZ), an overlapping zone within the spot weld center. The wire-cutting machine was used in cutting and preparing samples for testing the microstructure of dissimilar materials (pure Copper and AA6061-T6) to obtain a smooth cross-section. The examination used an optical microscope (OpitiKa) connected to a computer. Grinding paper (Sic) with different roughness numbers (800, 1000, 1500, 2000, 3000, and 4000) was used with distilled water to prepare the samples and then polished with a special cloth saturated with alumina solution with a volume of 0.5µm to obtain a polished surface ready for microstructure examination. An etching solution containing (0.3 ml distilled water + HCl 3.5ml+ HNO_3 4ml + CrO_3 1.2g) was used to examine the microstructure of the sample in various areas, such as the mixing area, the heat effect zone, and the base metal (Aluminum and Copper) with an immersion time of 30 sec. Figures 11 and 12 show images of the cross-section and microstructure of the various welding zones of the welding joint of the samples that gave the highest readings in the test of shear forces and under optimum conditions. As shown in Fig. 11 above, the distribution of areas on the weld sample, namely, Stir zone (SZ), Thermomechanical affect zone (TMAZ), Heat affect zone (HAZ), and Base metal (BM). Figure 12 displays images (a-g) of the sample microstructure in different areas along the interface of the sample cross-section, describing the state of bonding between the IL part and the lower sheet. The images show a clear difference in the microstructure between the base metals and the interlayer due to the pressure and temperature conditions during the welding process. Significantly larger dendritic growth was also formed in the stir zone. At the same time, the microstructure of the base mineral was coarser and larger. As a result of the difference in the granular size and to clearly show the microstructure of the interlayer, two magnification powers were used: 10x for the base metal and 20x for the interlayer. The area at the bottom of the IL-part fraction at the interface line with the bottom sheet is the recrystallization layer.

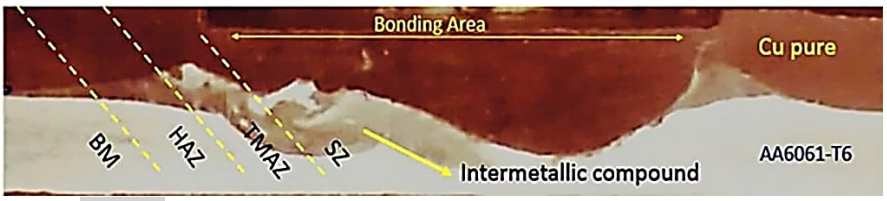

Fig. 11 Macroscopic Show of the Weld Sample Cross-Section.

The grain refinement can be seen in Fig. 11 (a-e), and it tends to form the dendritic as it gets closer to the stir zone because the materials in this area have undergone large amounts of plastic deformation, as shown in Fig. 12 (b-d). The base metal slightly changed its microstructure as the granules became soft in the mixing area. The change in the grain size for the intermediate layer in the SZ, TMAZ, HAZ, and BM are shown in Fig. 12. Images represent the C, D, and E stir areas (SZ). Dendritic growth of granules is formed. In Fig. 12 (a, b), small crystals are visible in the remainder of the sample cross-section. Dendritic growth can occur at recrystallization temperature upon rapid cooling [15]. The raised decrease in temperature formed dendrites, especially when the metal had a high ability to dissipate heat [33]. The dark-colored spots indicated in Fig 12 (a) indicate IMCs. To determine the intermetallic compound phases formed in the weld joint due to the mixing process between Copper and Aluminum, an examination was conducted by Scanning Electron Microscopy (SEM), Energy Dispersive X-ray Spectroscopy (EDS), and X-ray diffraction (XRD). These tests were conducted at Al-Khora Engineering Services Company, Yarmouk, Baghdad.

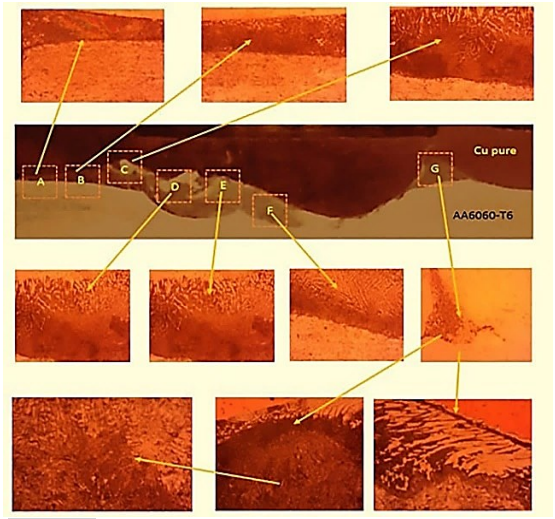

Fig. 12 Images Showing the Microstructure in Different Areas of the Examination Sample.

8.ANALYSIS OF EDS AND XRD RESULTS

For the analysis of intermetallic compounds, the EDS analysis was used. Figure 13 (a-c), respectively, shows the intermetallic compounds (IMCs) formed by mixing Al and Cu with the IL part, forming the Al/Cu intermetallic compound. The presence of the distinguished proportion of the O_2 in the EDS curves ensures the oxidation of the base metals. Points 2-4 show that Al was the main element found in these spots, which supports the fact that the IL part crashed downward under the movement action of the rotational tool. The presence of intermetallic compounds confirms an undoubted fact: metallurgical bonding between Aluminum and Copper. Figure 14 shows the X-ray diffraction patterns on the centerline of the weld cross-section. The results indicated that the basic components of welding consisted of intermetallic compounds, such as Al_2Cu, Al_3Cu_2, and Al_4Cu_9, along with quantities of Al and Cu. Conferring to the XRD results, the high frictional temperatures correlated with the stirring action caused by the mixing of Al and Cu heterogeneously, forming these intermetallic compounds, i.e., Al_2Cu, Al_3Cu_2, and Al_4Cu_9, meaning that a chemical reaction occurred between Al and Cu during welding. Complex, brittle intermetallic compounds between the dissimilar Joint of the Al and Cu were formed through the liquid state reaction, resulting from the excessive frictional heat generated and phase transformation [34, 35].

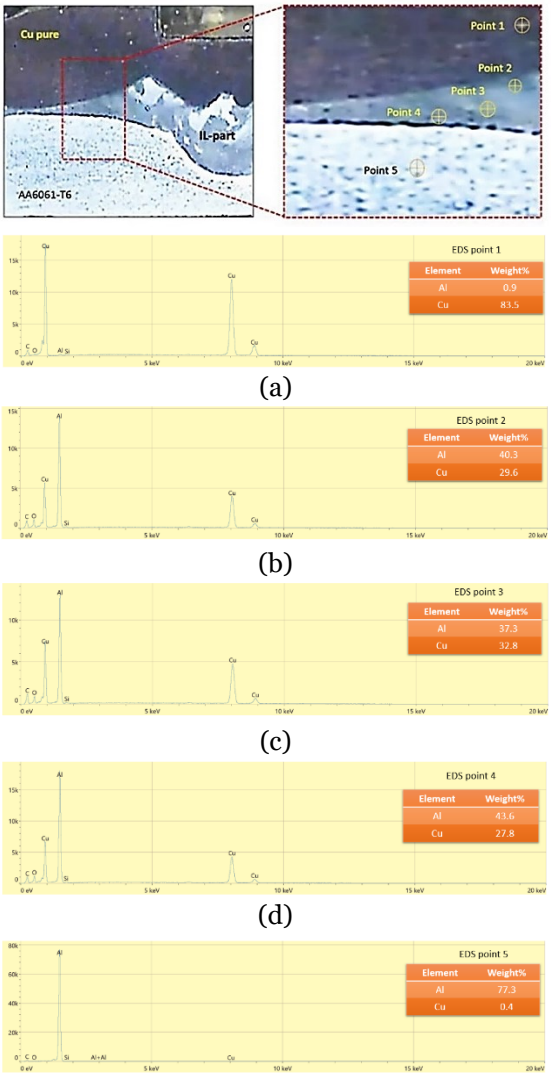

Fig. 13 EDS Analysis Results of the IL-FSSW Weld Joint.

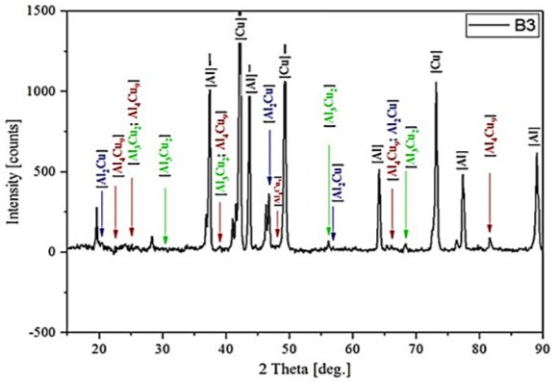

Fig. 14 X-ray Diffraction Patterns of the IL-FSSW.

9.FRACTURE MORPHOLOGY ANALYSIS

Figures 15 and 16 illustrate the fracture surfaces of the Aluminum and Copper sides of the welded joint under the shear-tensile test. The fracture morphologies were studied using SEM to understand the failure modes. Figures 15 (a) and 16 (a) show welding spots on the lower sheet (top surface) and upper sheet (bottom surface). In contrast, the other images show a magnification of the welding spot in different places (Center, edges) for Aluminum and Copper. Figures 15 (b-e) indicate the presence of dimples and micro-voids in the center of the welding spot and its edges. Their presence confirms the occurrence of failure under the shear fracture. Figure 16 (c) shows layers of ridges formed under the influence of stirring resulting from the movement of the welding tool. Figure 16 (d-e) displays high accuracy crystal boundaries and voids due to shear and tensile force dislocations. Based on the observations from the examination SEM, the fracture model for the Al-Cu joint made by the IL-FSSW process can be defined as a brittle fracture.

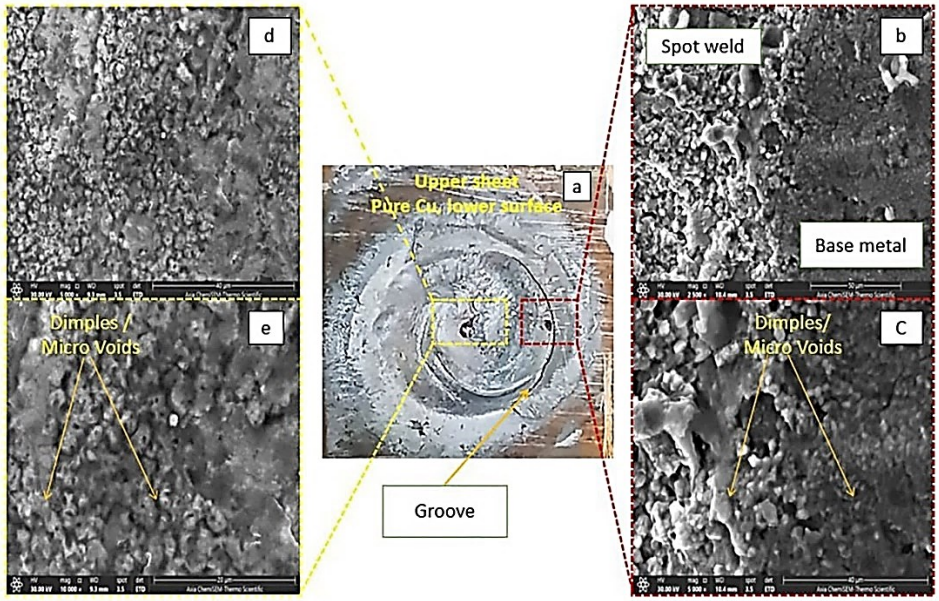

Fig. 15 SEM Inspection for the Lower Surface of the Upper Copper Sheet.

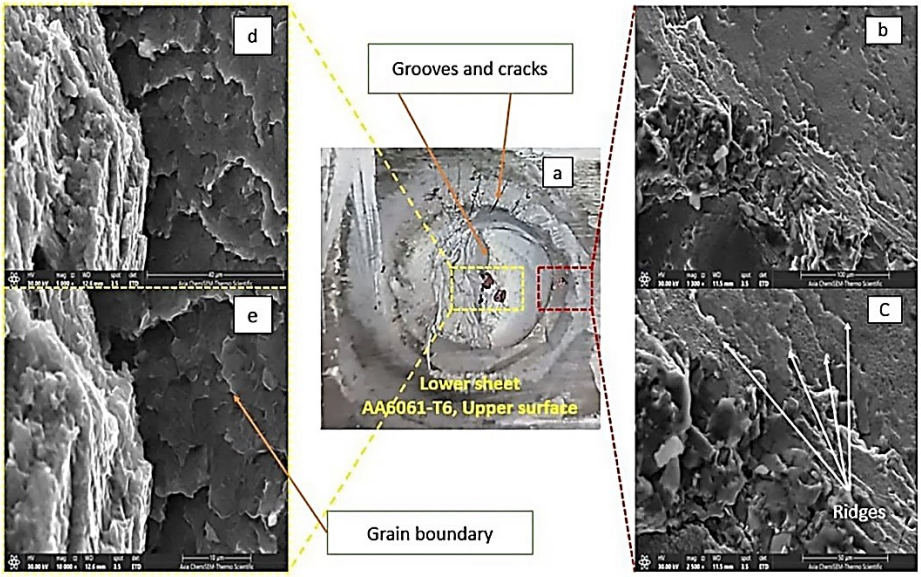

Fig. 16 SEM Inspection for the Upper Surface of the Aluminum Sheet 6061-T6.

10.CONCLUSION

In this paper, IL-FSSW was applied to weld Aluminum alloys with pure Copper. Below are the conclusions drawn from this study:

- Using an intermediate layer between Aluminum and Copper sheets obtained a joint that had a shallow keyhole.
- Using the intermediate layer noticeably increased the shear tensile strength of the joint compared with other methods.
- The base metal's microhardness value in the stir zone (SZ) increased noticeably, reaching 157Hv.
- Brittle intermetallic compounds formed due to the interaction of Aluminum and Copper led to a brittle fracture of the joint during tensile testing. The presence of intermetallic compounds is evidence of metallurgical bonding between Aluminum and Copper.
- The microstructure analysis revealed a difference in the size of the crystal grains between IL and base metal in the bonding zone and other areas. In the SZ region, dendritic grains were formed due to the metal's high potential for heat dissipation and, thus, rapid cooling, indicating the occurrence of recrystallization in this region. The dendritic granules hurt the mechanical properties of the joint, so they must be avoided.
- The Aluminum's low melting point and thermal conductivity compared to Copper led to the concentration of heat resulting from friction in the Aluminum sheet and its consumption in the annealing of the metal and the intermediate layer; this was the reason for the failure to achieve bonding in Group A-1, where there was not enough time for heat to reach the Copperplate and thus producing the weld joint.

ACKNOWLEDGMENTS

The authors extend their thanks and gratitude to all those who contributed to the achievement of this research, in particular the Department of Applied Mechanics at the Engineering Technical College-Baghdad, a Middle Technical University represented by its esteemed cadres.

REFERENCES

[1] Mohanraj N, Kumar NM, Prathap P, Ganeshan P, Raja K, Mohanavel V, Muhibbullah M. **Mechanical Properties and Electrical Resistivity of the Friction Stir Spot-Welded Dissimilar Al–Cu Joints**. *International Journal of Polymer Science* 2022; **2022**(1): 4130440, (1-7).

[2] Liu Hua, Zuo Yingying, Ji Shude, Dong Jihong, Zhao Huaxia. **Friction Stir Solid–Liquid Spot Welding of Cu to Al Assisted by Zn Interlayer**. *Journal of Materials Research and Technology* 2022; **18**:85-95.

[3] Galvão I, Loureiro A, Rodrigues DM. **Critical Review on Friction Stir Welding of Aluminium to Copper**. *Science and Technology of Welding and Joining* 2016; **21**(7):523-546.

[4] Badarinarayan H. **Fundamentals of Friction Stir Spot Welding**. Ph.D. Thesis. Missouri University of Science and Technology; Rolla, MO, USA: 2009.

[5] Saeid T, Abdollah-Zadeh AA, Sazgari B. **Weldability and Mechanical Properties of Dissimilar Aluminum–Copper Lap Joints Made by Friction Stir Welding**. *Journal of Alloys and Compounds* 2010; **490**(1-2):652-655.

[6] Ouyang J, Yarrapareddy E, Kovacevic R. **Microstructural Evolution in the Friction Stir Welded 6061 Aluminum Alloy (T6-Temper Condition) to Copper**. *Journal of Materials Processing Technology* 2006; **172**(1):110-122.

[7] Savolainen K. **Friction Stir Welding of Copper and Microstructure and Properties of the Welds**. Ph.D. Thesis. Aalto University; Otakaari 24, Finland: 2012.

[8] Handbook Metals. Metallography, Structures, and Phase Diagrams. ASTM, Metals Park, Ohio 1973.

[9] Akbari M, Abdi Behnagh R, Dadvand A. **Effect of Materials Position on Friction Stir Lap Welding of Al to Cu**. *Science and Technology of Welding and Joining* 2012; **17**(7):581-588.

[10] Wei H, Latif A, Hussain G, Heidarshenas B, Altaf K. **Influence of Tool Material, Tool Geometry, Process Parameters, Stacking Sequence, and Heat Sink on Producing Sound Al/Cu Lap Joints through Friction Stir Welding**. *Metals* 2019; **9**(8):875, (1-15).

[11] Manickam S, Rajendran C, Balasubramanian V. **Investigation of Fssw Parameters on Shear Fracture Load of Aa6061 and Copper Alloy Joints**. *Heliyon* 2020; **6**(6):e04077, (1-13).

[12] Regensburg A, Schürer R, Weigl M, Bergmann JP. **Influence of Pin Length and Electrochemical Platings on the Mechanical Strength and Macroscopic Defect Formation in Stationary Shoulder Friction Stir Welding of Aluminium to Copper**. *Metals* 2018; **8**(2):85, (1-9).

[13] Zykova A, Chumaevskii A, Gusarova A, Kalashnikova T, Fortuna S, Savchenko N,

Tarasov S. **Microstructure of in-Situ Friction Stir Processed Al-Cu Transition Zone**. *Metals* 2020; **10**(6):818.

[14] Chen S, Wang D, Li R, Liu B, Wang J. **Effect of a Zinc Interlayer on a Cu/Al Lap Joint in Ultrasound-Assisted Friction Stir Welding**. *Journal of Materials Engineering and Performance* 2019; **28**:5245-5254.

[15] Zhou L, Zhang RX, Li GH, Zhou WL, Huang YX, Song XG. **Effect of Pin Profile on Microstructure and Mechanical Properties of Friction Stir Spot Welded Al-Cu Dissimilar Metals**. *Journal of Manufacturing Processes* 2018; **36**:1-9.

[16] Zhou L, Li GH, Zhang RX, Zhou WL, He WX, Huang YX, Song XG. **Microstructure Evolution and Mechanical Properties of Friction Stir Spot Welded Dissimilar Aluminum-Copper Joint**. *Journal of Alloys and Compounds* 2019; **775**:372-382.

[17] Gao P, Zhang Y, Mehta KP. **Metallurgical and Mechanical Properties of Al–Cu Joint by Friction Stir Spot Welding and Modified Friction Stir Clinching**. *Metals and Materials International* 2021; **27**:3085-3094.

[18] Li M, Zhang C, Wang D, Zhou L, Wellmann D, Tian Y. **Friction Stir Spot Welding of Aluminum and Copper: A Review**. *Materials* 2019;**13**(1):156.

[19] Abed BH, Salih OS, Sowoud KM. **Pinless Friction Stir Spot Welding of Aluminium Alloy with Copper Interlayer**. *Open Engineering* 2020; **10**(1):804-813.

[20] Alaeibehmand S, Mirsalehi SE, Ranjbarnodeh E. **Pinless Fssw of Dp600/Zn/Aa6061 Dissimilar Joints**. *Journal of Materials Research and Technology* 2021; **15**:996-1006.

[21] Bajilane IJI. Development of a Solid State Spot Welding Technique for the Manufacturing of Detect Free Joints. Ph.D. Thesis. Özyeğin University; İstanbul, Turkey: 2019.

[22] Scott Jacqueline K. **Fracture Characteristics of Astm a-607 Pipe-Line Steel, Astm a-516 Structural Steel, and Astm B-209, Aluminum Alloys 5083 and 6061**. Construction Engineering Research Lab (Army) Champaign Ill; 1978: pp.

[23] Altman Jon C. **Hunter-Gatherers and the State: The Economic Anthropology of the Gunwinggu of North Australia**. Ph.D. Thesis. The Australian National University; Australia:1982.

[24] Kozina F, Zovko Brodarac Z, Jandrlić I, Jagustović R. **Analysis of the Crack Formation in Asis M2 High-Speed Tool Steel During Utilization**. *Proceedings book of 19th International Foundrymen Conference*: Sveučilište u Zagrebu Metalurški fakultet; 2021.

[25] de Castro CC, Plaine AH, de Alcântara NG, dos Santos JF. **Taguchi Approach for the Optimization of Refill Friction Stir Spot Welding Parameters for Aa2198-T8 Aluminum Alloy**. *The International Journal of Advanced Manufacturing Technology* 2018; **99**:1927-1936.

[26] Society American Welding. Journal of the American Welding Society 1929; **8**: American Welding Society; 1929.

[27] Pan Tsung-Yu. **Friction Stir Spot Welding (FSSW)-A Literature Review**. 2007.

[28] Ibrahim IJ, Yapici GG. **Application of a Novel Friction Stir Spot Welding Process on Dissimilar Aluminum Joints**. *Journal of Manufacturing Processes* 2018; **35**:282-288.

[29] Ibrahim IJ, Yapici GG. **Optimization of the Intermediate Layer Friction Stirs Spot Welding Process**. *The International Journal of Advanced Manufacturing Technology* 2019; **104**: 993-1004.

[30] Zuo YY, Gong P, Ji SD, Li QH, Ma ZW, Lv Z. **Ultrasound-Assisted Friction Stir Transient Liquid Phase Spot Welded Dissimilar Copper-Aluminum Joint**. *Journal of Manufacturing Processes* 2021; **62**:58-66.

[31] Abbass MK, Hussein SK, Kudair AA. **Optimization and Characterization of Friction Stir Spot Welding of Aluminum Alloy (Aa 5754-H114) with Pure Copper Sheet**. *IOP Conference Series: Materials Science and Engineering*: IOP Publishing; 2021. pp. 012054.

[32] Davis Joseph R. **Metals Handbook Desk Edition**. 1998.

[33] Siddharth S, Senthilkumar T. **Study of Tool Penetration Behavior in Dissimilar Al5083/C10100 Friction Stir Spot Welds**. *Procedia Engineering* 2017; **173**:1439-1446.

[34] Aravind M, Yu P, Yau M Yu, Ng Dickon HL. **Formation of Al2cu and Alcu Intermetallics in Al (Cu) Alloy Matrix Composites by Reaction Sintering**. *Materials Science and Engineering:* 2004; **380**(1-2):384-393.

[35] Dawood HI, Mohammed Kahtan S, Rahmat Azmi, Uday MB.

Microstructural Characterizations and Mechanical Properties in Friction Stir Welding Technique of Dissimilar (Al-Cu) Sheets. *Journal of Applied Science and Agriculture* 2015; **10**(5):149-158.